Asian Journal of Atmospheric Environment
Vol. 11, No. 2, pp. 114-121, June 2017
doi: https://doi.org/10.5572/ajae.2017.11.2.114
ISSN (Online) 2287-1160, ISSN (Print) 1976-6912

Temporal Variation of Atmospheric Radon-222 and Gaseous Pollutants in Background Area of Korea during 2013-2014

Jun-Oh Bu, Jung-Min Song, Won-Hyung Kim, Chang-Hee Kang*, Sang-Keun Song[1)], Alastair G. Williams[2)] and Scott D. Chambers[2)]

Department of Chemistry and Cosmetics, College of Natural Sciences, Jeju National University, Jeju 63243, Republic of Korea
[1)]Department of Earth and Marine Sciences, College of Ocean Sciences, Jeju National University, Jeju 63243, Republic of Korea
[2)]Australian Nuclear Science and Technology Organisation, Locked Bag 2001, Kirrawee DC, NSW 2232, Australia

*Corresponding author. Tel: +82-64-754-3545, E-mail: changhee@jejunu.ac.kr

ABSTRACT

Real-time monitoring of hourly concentrations of atmospheric Radon-222 (^{222}Rn, radon) and some gaseous pollutants (SO_2, CO, O_3) was performed throughout 2013-2014 at Gosan station of Jeju Island, one of the cleanest regions in Korea, in order to characterize their background levels and temporal variation trend. The hourly mean concentrations of radon and three gaseous pollutants (SO_2, CO, O_3) over the study period were 2216±1100 mBq/m^3, 0.6±0.7 ppb, 211.6±102.0 ppb, and 43.0±17.0 ppb, respectively. The seasonal order of radon concentrations was as fall (2644 mBq/m^3) ≈ winter (2612 mBq/m^3) > spring (2022 mBq/m^3) > summer (1666 mBq/m^3). The concentrations of SO_2 and CO showed similar patterns with those of radon as high in winter and low in summer, whereas the O_3 concentrations had a bit different trend. Based on cluster analyses of air mass back trajectories, the air mass frequencies originating from Chinese continent, North Pacific Ocean, and the Korean Peninsula routes were 30, 18, and 52%, respectively. When the air masses were moved from Chinese continent to Jeju Island, the concentrations of radon and gaseous pollutants (SO_2, CO, O_3) were relatively high: 2584 mBq/m^3, 0.76 ppb, 225.8 ppb, and 46.4 ppb. On the other hand, when the air masses were moved from North Pacific Ocean, their concentrations were much low as 1282 mBq/m^3, 0.24 ppb, 166.1 ppb, and 32.5 ppb, respectively.

Key words: Radon-222, Gaseous pollutants, Air mass pathway, Gosan station, Back trajectory

1. INTRODUCTION

Radon-222 is a gaseous decay product of uranium (^{238}U), which is ubiquitous in most rock and soil types and distributes roughly universally throughout the crust (Omori *et al*., 2009). As radon is poorly soluble and does not react chemically with another elements, therefore its origin is restricted almost entirely to land surfaces. It has a relatively short half-life of 3.8 days, and since terrestrial radon fluxes are 2-3 orders of magnitude greater than oceanic fluxes, there is a large contrast between radon concentrations in continental and aged oceanic air masses. Consequently, radon monitoring at island or coastal sites provides insight into air mass history including the extent of recent land contact. This is a desirable characteristic since most anthropogenic atmospheric pollutants are also of terrestrial origin.

In the atmosphere, gaseous ^{222}Rn generates short-lived (^{218}Po, ^{214}Pb, ^{214}Bi, and ^{214}Po) and long-lived (^{210}Pb, ^{210}Bi, and ^{210}Po) radioactive decay products, which are chemically reactive and readily become attached to airborne particulate matter (Song *et al*., 2015). Most inhaled radon is exhaled and relatively few alpha particles are emitted in the body. However, radon produces four immediate decay products, which have short half-lives and are all radioactive isotopes of solid elements (Bu *et al*., 2016). The decay products, attached to the surface of aerosols, dust, smoke, and moisture particles, may remain in the respiratory system and eventually lead to lung cancer (Miles, 1998).

Radon is inert, and relatively unsusceptible to wet or dry atmospheric removal processes, so its predominant atmospheric sink is radioactive decay. Since the half-life is comparable to the lifetimes of short-lived atmospheric pollutants (e.g. NO_x, SO_2, CO, O_3) and the residence times of water and aerosols, radon is a particularly useful tracer at local, regional or global scales (Kang *et al*., 2007; Zahorowski *et al*., 2005, 2004; Taguchi *et al*., 2002). Radon's unique characteristics also make it a useful indicator of vertical mixing as well as the influence of changing atmospheric mixing depth on

near-surface observations of urban emissions. Therefore, continuous monitoring of radon and various atmospheric pollutants could be positively encouraged to understand the atmospheric dilution effects on precursor species from Asia continent by the prevailing westerlies (Song *et al*., 2015; Chambers *et al*., 2014). Furthermore, radon observations at World Meteorological Organization/Global Atmospheric Watch (WMO/GAW) monitoring stations constitute a powerful tool for identifying "baseline" (hemispheric background) air masses (Chambers *et al*., 2014), which is crucial for advancing our understanding of the relationship between long-term changes in atmospheric composition and changes in global and regional climate, as well as the long range atmospheric transport and deposition of potentially harmful substances over a range of ecosystems (IAEA/WMO, 2012; Zhang *et al*., 2011; WMO/GAW, 2001).

Due to a rapid industrial development as well as an expanding dissemination of the Asian dust, the amount of atmospheric pollutants has been gradually produced in the Northeast Asia year by year. Especially, due to a long-range transport of atmospheric pollutants, the falling amounts of various acidic substances have increased in Korea and Japan which are geographically located at a near distance from the coastal industry area of northeastern China and situated downwind by the prevailing westerly wind (Bu *et al*., 2016; Kim *et al*., 2013; Takami *et al*., 2007). As Jeju Island is one of the background areas in Korea and contributes comparatively little to the regional air pollution, it is the optimal place to observe the outfolw of air pollutants emitted in the East Asian region. In particular, Gosan station, which is located on the western extremity of Jeju Island, has been the focal point of several major initiatives pertaining to regional air quality and understanding the climatic effects of atmospheric aerosols. It is a long-term monitoring facility for various air quality parameters and atmospheric radon. Some various air quality monitoring programs have been in operation at Gosan station since the early 1990s, and also continuous hourly radon monitoring has been performed since 2001 (Bu *et al*., 2016; Han and Huh, 2014; Huebert *et al*., 2003).

In this study, the background levels of atmospheric radon concentrations and their temporal variations on diurnal to seasonal time-scales were characterized based on the monitoring data performed at Gosan station for two years during 2013-2014. In addition, we have attempted to overview and characterize the timely variation of radon and gaseous pollutants such as SO_2, CO, and O_3, monitored at the same place, in accordance with the transport pathways of air masses.

2. MATERIALS AND METHODS

2.1 Monitoring Site

Real-time monitoring of atmospheric radon was performed at Gosan station (33.17°N, 126.10°E), which is situated on the western extremity of Jeju Island in Korea. Jeju Island is located approximately 500 km east from the east coastline of China, 300 km west from Kyushu of Japan, and 100 km south from the Korean Peninsula. Gosan is one of the background sites in Korea, which contributes comparatively little to the regional air pollution, and Gosan station is situated on the coast, near the edge of a seashore cliff approximately 72 m above sea level. Consequently, it is a quite suitable site to observe the long-range transport of air pollutants and transformation of ambient trace species in the northeast Asia region, and also the impact of continental outflow events (Song *et al*., 2015; Kim *et al*., 2013).

2.2 Atmospheric Radon Monitoring

The continuous hourly atmospheric radon monitoring was made at Gosan station from January 2013 to December 2014 using a 1500 L dual-flow-loop/two filter radon detector (model D1500). The radon detector was designed and built at the Australian Nuclear Science and Technology Organization (ANSTO), and then installed at Gosan station, as shown in Fig. 1. This detector provides a direct measurement of the ambient atmospheric radon concentration that is independent of the concentration of radon progeny in the atmosphere or the level of equilibrium established between radon and its progeny. The operation principle of this detector model has been documented by Whittlestone and Zahorowski (1998), etc. (Bu *et al*., 2016; Song *et al*., 2015; Chambers *et al*., 2011; Whittlestone and Zahorowski, 1998).

For the study, the air flow rate was approximately 50 L/min through a 50 mm High-Density Polyethylene intake line, and the height of the air inlet was 10 m above ground level. The response time of the detector was about 45 minutes, and the lower limit of detection was approximately 30 mBq/m^3. The calibration of the radon detector had been carried out on a monthly basis by injecting radon gas for 5 hours from a Pylon source ($18.5 \pm 4\%$ kBq Radium-226) traceable to National Institute of Standards and Technology standards. The instrumental background had been checked every 3 months for its subtraction from the raw data. The raw radon counts and all detector diagnostic parameters were recorded every 30 minutes using a Campbell Scientific data logger (CR800), and transferred to the controlling computer. The half-hourly data were subsequently aggregated to the hourly values after calibra-

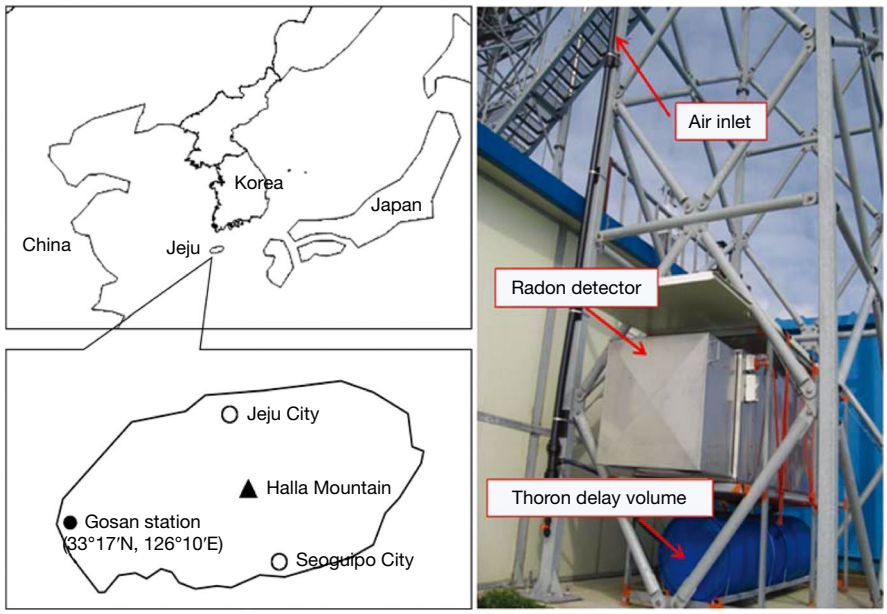

Fig. 1. Location of Gosan station at Jeju Island and installation of the 1500 L radon detector (ANSTO, D1500).

tion and quality checks. The time scale used throughout this study is local standard time (LST = UTC + 9 h).

2. 3 Gaseous Pollutants Measurement

The continuous hourly concentrations of gaseous atmospheric pollutants have been measured at Gosan station by the Korean Ministry of Environment, and we focused only on the short-lived atmospheric pollutants: sulfur dioxide (SO_2), carbon monoxide (CO), and ozone (O_3), for being comparable to the lifetime of radon and also used as indicators of anthropogenic activity. For the monitoring of these gaseous pollutants, the measurement of SO_2 was made by using UV fluorescence (Thermo Environmental Instruments, model 43C-TL, USA). On the other hand, CO and O_3 were measured by Non-Dispersive Infrared absorption (Thermo Environmental Instruments, model 48C, USA) and UV photometric method (Thermo Environmental Instruments, model 49C, USA), respectively (Chambers *et al*., 2015).

2. 4 Air Mass Back Trajectories

Typical air-flow patterns can be derived from back trajectory analysis. Air mass back trajectories for this study were calculated using the PC version of HYSPLIT 4.0 (HYbrid Single-Particle Lagrangian Integrated Trajectory) supplied by NOAA/ARL (National Oceanic and Atmospheric Administration/Air Resources Laboratory) (Draxler and Rolph, 2013). HYSPLIT usually calculates back trajectories using meteorological data of 1° × 1° resolution generated by the global data assimilation system (GDAS) model from the National Weather Service's (NWS) National Centre for Environmental Prediction (NCEP) (Draxler, 1999). The 72-hour back trajectories were calculated starting from Gosan station (33.17°N, 126.10°E) at an altitude of 500 m above ground level. This altitude has been chosen such that the starting height is typically within the marine boundary layer (MBL), which varies seasonally at Gosan area from 300 to 1200 m, and it is high enough not to be affected by the local terrain.

3. RESULTS AND DISCUSSION

3. 1 Variation Characteristics of Radon and Gaseous Pollutants

Hourly concentrations of atmospheric radon were measured at Gosan station using a real-time radon detector system for two years during 2013-2014. The hourly radon time-series for this study period is presented in Fig. 2. In this study, the hourly and daily mean radon concentrations were 2216 ± 1100 mBq/m^3 and 2226 ± 859 mBq/m^3, respectively. These radon levels are two or three times higher than those measured at Seoul (7620 mBq/m^3) and Hok Tsui (Hong Kong; 5580 ± 626 mBq/m^3). At Mauna Loa, however, where air can be sampled further from the surface within the lower troposphere, hourly mean radon concentrations (106 mBq/m^3) were about 20.9 times lower than observed at Gosan (Chambers *et al*., 2013; Chambers *et al*., 2009; Zahorowski *et al*., 2005).

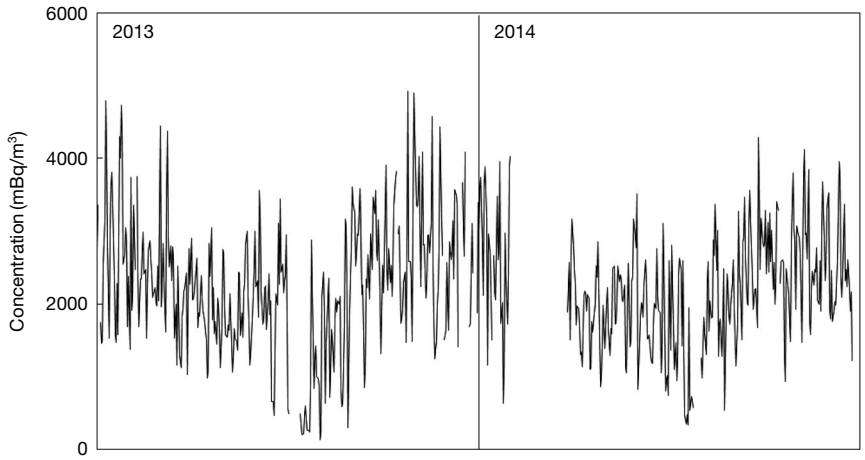

Fig. 2. Yearly time-series variation of atmospheric radon concentrations measured at Gosan station during 2013-2014.

From the seasonal comparison, the time-series radon concentration at Gosan shows a repeated seasonal variability. The seasonal mean radon concentrations were in the order of fall (2644 mBq/m^3) ≈ winter (2612 mBq/m^3) > spring (2022 mBq/m^3) > summer (1666 mBq/m^3). The seasonal cycle of radon was characterized by a winter maximum and summer minimum, consistent with the reduction in terrestrial fetch from winter to summer (Fig. 3). Seasonal change in radon concentration at Gosan is typically driven by monsoon-related variability in wind direction. During the winter monsoon, air flow in the lower atmosphere is directed from north and west; the reverse occurs in summer (Bu *et al*., 2016; Song *et al*., 2015).

At Gosan, seasonal mean of the radon concentration indicates the potential for influence from large-scale terrestrial-based sources, whereas diurnally, radon concentrations respond to the changing local mixing depth. Therefore it demonstrates a decreasing potential for large-scale pollution contributions from winter to summer, and corresponding increase in the potential for contamination of observations by local-scale emissions as diurnal mixing depth changes become more pronounced (Bu *et al*., 2016; Chambers *et al*., 2011).

Throughout the winter monsoons, regional flow of air mass is usually north-westerly to northerly in Jeju Island. While throughout the summer monsoon, regional flow is often south-easterly and wind speeds are approximately half their winter values. In summer, the amplitude of the diurnal radon cycle usually well exceeds the daily mean value, indicating that, on average, there was a significant marine influence on mixing depths at Gosan. However, amplitude of the diurnal radon cycle and mixing depths at Gosan in spring and fall lies between the winter and summer extremes

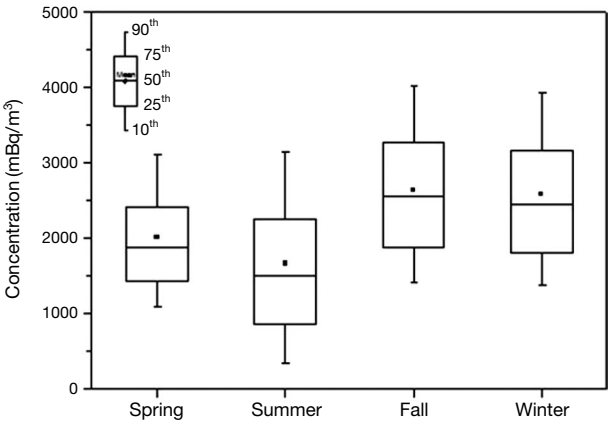

Fig. 3. Seasonal comparison of radon concentrations (10th/25th/50th/75th/90th percentiles) at Gosan station.

(Fig. 4).

Similarly, the seasonal concentrations of SO_2 and CO were high for the winter season, whereas the concentrations for the summer season have a low measured value. In the case of O_3, unlike other gaseous components, the seasonal concentration was high in spring and low in summer. To investigate the possibility of similar local influences on observations of criteria pollutants at Gosan we analyzed diurnal composite plots of CO and SO_2. As was observed for radon, the diurnal cycle of CO concentrations was characterized by a morning maximum, afternoon minimum, and nocturnal build-up phase. The diurnal cycle of SO_2, is completely out of phase with that of the CO observations; exhibiting maximum values around noon, and minimum concentrations during the night. This contrast can be readily explained by the diurnal mixing

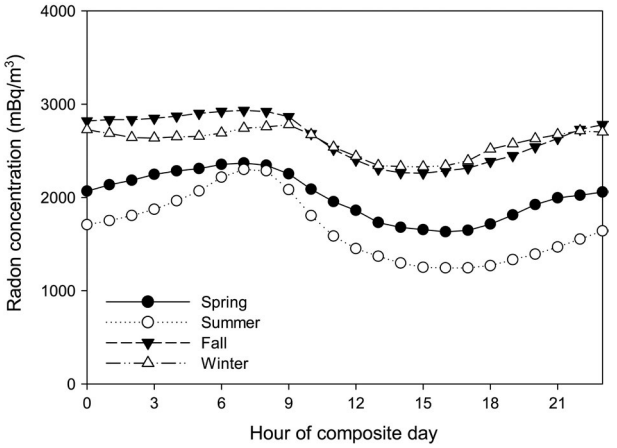

Fig. 4. Diurnal pattern of hourly radon concentrations by seasons at Gosan station.

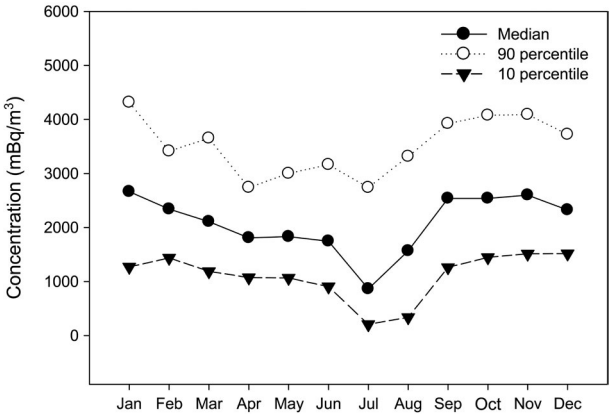

Fig. 5. Distribution (10^{th}/50^{th}/90^{th} percentiles) of mean monthly radon concentration at Gosan station.

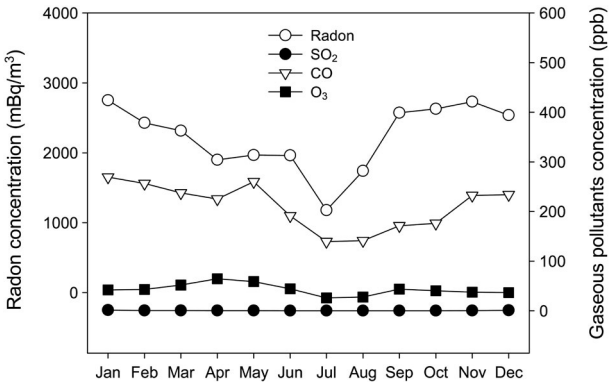

Fig. 6. Monthly comparison of radon and gaseous pollutants concentrations.

patterns and contrasting CO/SO_2 source characteristics of the Gosan fetch.

In descending order of magnitude, the monthly mean radon concentrations were January > November > October > September > December > February > March > May > June > April > August > July over the study periods (Fig. 5). The highest monthly radon concentration, 2752 mBq/m^3 in January, was more than twice the lowest value, 1178 mBq/m^3 in July. From the monthly comparison, the radon concentrations are observed highly from September through March, during the period of most consistent terrestrial fetch due to the strong northerly component of wind direction and dry air masses for the height of the Asian winter monsoon. On the other hand, the lowest radon concentrations were typically measured between July and August, indicating the lowest land influence, during the period of relatively dominant oceanic fetch due to the strong southerly wind component and wet air masses (Bu *et al.*, 2016).

The monthly concentration variations of radon and gaseous pollutants (SO_2, CO, O_3) are shown in Fig. 6. In continental regions, sulfur dioxide results mainly from fossil fuel combustion, therefore it is considered to be one of the most important precursor components for secondary matter in the atmosphere. The oxidation of sulfur dioxide leads to the production of sulfuric acid, and its atmospheric lifetime with respect to oxidation is typically a few days. However, the rate of oxidation is variable, since it may occur both in aqueous droplets, and in the gaseous phase where the sulphuric acid itself may condense to form condensation nuclei. Carbon monoxide is emitted into the atmosphere as a result of incomplete combustion processes, and is also formed from the oxidation of hydrocarbons and other organic compounds. The highest concentrations are found close to combustion sources, and atmospheric lifetime for further oxidation to form carbon dioxide is comparable to radon, enabling long-range transport.

The formation of ozone requires the presence of three ingredients: hydrocarbons, nitrogen oxides and sunlight. Consequently, high levels of ozone are generally observed under sunny, summertime conditions in locations where the air mass has previously collected emissions of hydrocarbons and nitrogen oxides. Ozone plays an important role in controlling the chemical composition of the troposphere. O_3 is also produced and destroyed within the troposphere by chemical reactions involving free radicals. It is formed during the oxidation of CO, CH_4, and hydrocarbons in the presence of nitrogen oxides and destroyed by reactions with HO_X radicals.

During the study period, the monthly SO_2 and CO concentrations showed the highest values in January.

However, their concentrations for summer season (July, August) were lower than 6.4 times and twice, respectively, compared to the highest concentrations. Meanwhile, the highest monthly O_3 concentration, 64.5 ppb in April, was more 2.5 times than the lowest value, 26.1 ppb in July. Consequently, the monthly radon and gaseous pollutants concentrations were affected by the seasonal wind directions.

3.2 Fetch Effects on Atmospheric Radon and Gaseous pollutants

The ability to reliably characterize air mass fetch regions is of critical importance to the thorough interpretation of aerosol and trace gas samples collected at any site (Zahorowski *et al*., 2005). Much of the more recent active interest in environmental radon monitoring can be attributed to its peculiar characteristics as a tracer of atmospheric processes (Song *et al*., 2015). There are several proposals about radon flux distributions in the local, regional or global scale using various methods (Rogers and Nielson, 1991). Specially, as mentioned earlier, radon is poorly soluble and unreactive, and its predominant sink is by radioactive decay. The half-life of radon is comparable to the lifetimes of short-lived atmospheric pollutants (e.g. NO_X, SO_2, CO, O_3) and the atmospheric residence time of water and aerosols, and is comparable to many important aspects of atmospheric dynamics (Song *et al*., 2015). Because of its short residence time in the atmosphere and wide range of surface emanation rates, the interpretation of radon measurements is highly site-specific. Radon has been routinely measured at both continental and remote global sites, and long range transport sudies are best made from coastal or high-altitude sites free of local radon source (Bu *et al*., 2016; GAW, 2001).

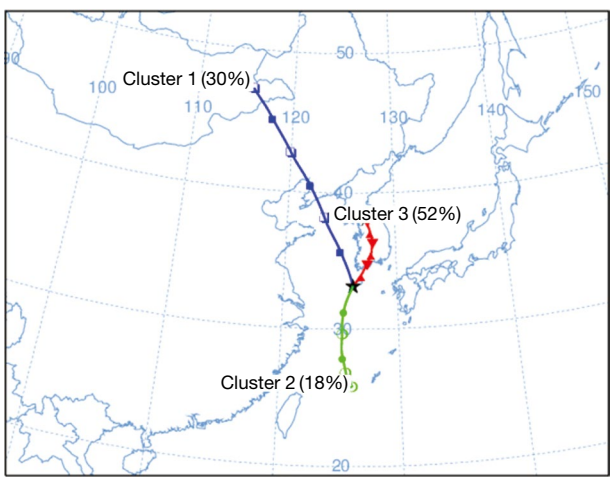

Fig. 7. Three inflow pathway types of air masses classified by clustered back trajectory analysis.

To identify the terrestrial portions of the China and Korea fetch regions that had the greatest influence on Gosan air quality observations, clusters of back trajectories were generated corresponding to air masses with the radon concentrations. For the study periods, cluster analysis of the air mass back trajectories was investigated in order to know the influence of air mass transport pathways on the variability of radon and gaseous pollutants concentrations at Gosan station (Fig. 7). Trajectories from 638 days could be grouped into three clusters. The dominant fetch regions were well represented by the cluster groups, which were associated with clearly distinct air quality statistics, were: Cluster 1 (Chinese continent), Cluster 2 (The North Pacific Ocean), and Cluster 3 (Korean Peninsula). During the study periods, the classification of air mass fetch by transport pathways were Cluster 1 (30%; 194 days), Cluster 2 (18%; 113 days), and Cluser 3 (52%; 331 days).

The concentrations of radon and gaseous pollutants (SO_2, CO, and O_3) were compared in accordance with the air mass pathways, as shown in Fig. 8 and Table 1. Their concentrations were in order of Cluster 1 > Cluster 3 > Cluster 2 during the study periods, showing the highest when the air masses have moved from the Chinese continent, but low when the air masses come from the North Pacific Ocean. Also it was evident that

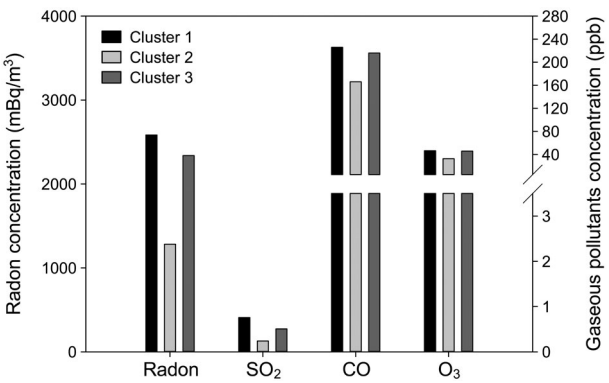

Fig. 8. Concentrations of atmospheric radon and gaseous pollutants in relation to three inflow pathway types of air masses.

Table 1. Concentrations of radon and gaseous pollutants corresponding to clustered back trajectories.

Group	Radon (mBq/m^3)	Gaseous pollutants (ppb)		
		SO_2	CO	O_3
Cluster 1	2584	0.76	225.8	46.4
Cluster 2	1282	0.24	166.1	32.5
Cluster 3	2338	0.51	216.0	45.8

the variation trend of radon concentrations had a quite similar pattern with those gaseous pollutants in three clustered trajectories.

4. CONCLUSION

Real-time monitoring of hourly concentrations of atmospheric radon and gaseous pollutants (SO_2, CO, O_3) was performed throughout 2013-2014 at Gosan station of Jeju Island, to characterize the temporal variation. The hourly mean radon concentrations were 2216 ± 1100 mBq/m^3. The radon, SO_2, and CO showed a high concentration in the winter seasons, when air mass pathways were prevailing in northwestly wind direction. Meanwhile, the concentration of O_3 was high in spring seasons, and it should be confirm the concentrations of ozone precursors to examine the exact cause. From the comparison of radon and gaseous pollutants by clustered back trajectory analysis, the concentrations of all those species were in order of Cluster 1 (Chinese continent) > Cluster 3 (Korean Peninsula) > Cluster 2 (The North Pacific Ocean), showing the significant impact of the China continent. Furthermore, it was found that the concentrations of radon and gaseous pollutants increase highly when the air masses have moved from the China continent, on the other hand, their concentrations relatively decrease when the air masses come from the North Pacific Ocean.

ACKNOWLEDGEMENT

This work was funded by the Korea Meteorological Administration Research and Development Program under Grant KMIPA 2015-2050.

REFERENCES

Bu, J.O., Song, J.M., Kim, W.H., Kang, C.H., Chambers, S.D., Williams, A.G., Lee, C. (2016) Variability of Atmospheric Radon-222 and Secondary Aerosol Components in Accodance with Air Mass Transport Pathways at Jeju Island, Korea, during 2011-2014. Bulletin of the Korean Chemical Society 37, 841-846.

Chambers, S.D., Williams, A.G., Crawford, J., Griffiths, A.D. (2014) On the use of radon for quantifying the effects of atmospheric stability on urban emissions. Atmospheric Chemistry and Physics Discussions 14, 25411-25452.

Chambers, S.D., Kang, C.H., Williams, A.G., Crawford, J., Griffiths, A.D., Kim, K.H., Kim W.H. (2015) Improving the Representation of Cross-Boundary Transport of Anthropogenic Pollution in East Asia Using Radon-222. Aerosol and Air Quality Research, 1-19.

Chambers, S.D., Williams, A.G., Crawford, J., Griffiths, A.D., Krummel, P.B., Steels, L.P., Galbally, I.E., Molloy, S., van der Schoot, M.V. (2014) A radon-only technique for characterising baseline constituent concentrations at Cape Grim. In Atmospheric Composition & Modelling Conference incorporating the Cape Grim Annual Science Meeting 2014, Aspendale, Victoria, Australia.

Chambers, S., Williams, A.G., Zahorowski, W., Griffiths, A., Crawford, J. (2011) Separating remote fetch and local mixing influences on vertical radon measurements in the lower atmosphere. Tellus 63B, 843-859.

Chambers, S., Zahorowski, W., Matsumoto, K., Uematsu, M. (2009) Seasonal variability of radon-derived fetch regions for Sado Island, Japan, based on 3 years of observations: 2002-2004. Atmospheric Environment 43, 271-279.

Chambers, S.D., Zahorowski, W., Williams, A.G., Crawford, J., Griffiths, A.D. (2013) Identifying tropospheric baseline air masses at Mouna Loa Observatory between 2004 and 2010 using Radon-222 and back trajectories. Journal of Geophysical Research 118, 992-1004.

Draxler, R.R. (1999) HYSPLIT_4 User's Guide, NOAA Technical Memorandum ERL ARL-230, 35 pp (http://ready. arl.noaa.gov/HYSPLIT.php).

Draxler, R.R., Rolph, G.D. (2013) HYSPLIT (Hybrid Single-Particle Lagrangian Intergrated Trajectory) Model access via NOAA ARL READY Website (http://ready. arl.noaa.gov/ HYSPLIT_traj. php).

Han, Y., Huh, Y. (2014) Assessing the Inpact of Locally Produced Aerosol on the Rainwater Composition at the Fosan Background Site in East Asia. Asian Journal of Atmospheric Environment 8, 69-80.

Huebert, B.J., Bates, T., Russell, P.B., Shi, G., Kim, Y.J., Kawamura, K., Carmichael, G., Nakajima, T. (2003) An overview of ACE-Asia: Strategie for quantifying the relationships between Asian aerosols and their climatic impacts. Journal of Geophysical Research 108, 8633, doi:10.1029/2003JD003550.

IAEA/WMO (2012) Sources and Measurements of Radon and Radon Progeny Applied to Climate and Air Quality Studies: IAEA Proceeding Series, International Atomic Energy Agency, Vienna International Centre, p. 9.

Kang, C.H., Ko, H.J., Zahorowski, W. (2007) Radon and TSP Concentrations in the Ambient Air of Gosan Area, Jeju Island between 2001 and 2004. Journal of Korean Society for Atmospheric Environment 23, 612-624.

Kim, W.H., Hwang, E.Y., Ko, H.J., Kang, C.H. (2013) Seasonal Composition Characteristics of TSP and $PM_{2.5}$ Aerosols at Gosan Site of Jeju Island, Korea during 2008-2011. Asian Journal of Atmospheric Environment 7, 217-226.

Miles, J. (1998) Development of maps of radon-prone areas using radon measurements in houses. Journal of Hazardous Materials 61, 53-58.

Omori, Y., Tohbo, I., Nagahama, H., Ishikawa, Y., Takahashi, M., Sato, H., Sekine, T. (2009) Variation of

atmospheric radon concentration with bimodal seasonality. Radiation Measurements 44, 1045-1050.

Rogers, V.C., Nielson, K.K. (1991) Multiphase Radon Generation and Transport in Porous Materials. Health Physics 60, 807-815.

Song, J.M., Kim, W.H., Kang, C.H., Lee, H., Lee, C., Chambers, S., Williams, A.G. (2015) Temporal Variability of Atmospheric Radon-222 Concentration at Gosan Station, Jeju Island, Korea, during 2009-2013. Bulletin of the Korean Chemical Society 36, 603-608.

Taguchi, S., Iida, T., Morizumi, J. (2002) Evaluation of the atmospheric transport model NIRE-CTM-96 by using measured radon-222 concentrations. Tellus 54B, 250-268.

Takami, A., Miyoshi, T., Shimono, A., Kaneyasu, N., Kato, S., Kajii, Y., Hatakeyama, S. (2007) Transport of anthropogenic aerosols from Asia and subsequent chemical transformation. Journal of Geophysical Research 112, D22S31, doi:10.1029/2006JD008120.

Whittlestone, S., Zahorowski, W. (1998) Baseline radon detectors for shipboard use: Development and deployment in the First Aerosol Characterization Experiment (ACE 1). Journal of Geophysical Research 103, 16743-16751.

WMO/GAW (2001) Global Atmosphere Watch Measurements Guide (No. 143), WMO TD No. 1073, p. 55.

WMO's Global Atmosphere Watch (GAW) (2001) Global Atmosphere Watch Measurements Guide (WMO TD No. 1073), p 55.

Zahorowski, W., Chambers, S.D., Henderson-Sellers, A. (2004) Ground based radon-222 observations and their application to atmospheric studies. Journal of Environmental Radioactivity 76, 3-33.

Zahorowski, W., Chambers, S., Wang, T., Kang, C.H., Uno, I., Poon, S., Oh, S.N., Werczynski, S., Kim, J., Henderson-Sellers, A. (2005) Radon-222 in boundary layer and free tropospheric continental outflow events at three ACE-Asia sites. Tellus 57B, 124-140.

Zhang, K., Feichter, J., Kazil, J., Wan, H., Zhuo, W., Griffiths, A.D., Sartorius, H., Zahorowski, W., Ramonet, M., Schmidt, M., Yver, C., Neubert, R.E.M., Brunke, E.-G. (2011) Radon activity in the lower troposphere and its impact on ionization rate: a global estimate using different radon emissions. Atmospheric Chemistry and Physics 11, 7817-7838.

(Received 20 February 2017, revised 11 May 2017, accepted 1 June 2017)